

Anneke Hibma · Henk M. Schuttelaars
Zheng B. Wang

Comparison of longitudinal equilibrium profiles of estuaries in idealized and process-based models

Received: 1 November 2002 / Accepted: 5 June 2003
© Springer-Verlag 2003

Abstract The process-based morphodynamic model Delft3D-MOR and the idealized model of Schuttelaars and De Swart (2000) are compared with each other. The differences between the two models in their mathematical-physical formulation as well as the boundary conditions are identified. Their effect on producing cross-sectionally averaged morphological equilibria of tidal inlets with arbitrary length and forced at the seaward boundary by a prescribed M_2 and M_4 sea-surface elevation is studied and an inventory is made of all relevant differences. The physical formulations in the source code of Delft3D-MOR are modified in various steps to resemble the formulations in the idealized model. The effect of each of the differences between the idealized and process-based model are studied by comparing the results of the idealized model to those of the adapted process-based model. The results of the idealized model can be qualitatively reproduced by the process-based model as long as the same morphological boundary condition is applied at the open sea end. This means that the simplifications concerning the mathematical formulation of the physical processes in the idealized model can be justified. Furthermore, it can be inferred that the morphological boundary condition at the open sea end is an essential element in controlling the behaviour of morphodynamic models for tidal inlets and estuaries.

Keywords Tidal basin · Estuaries · Morphology · Numerical model · Idealized model · Morphodynamic equilibrium

1 Introduction

Tidal inlets are observed in many coastal areas all over the world. The length of these inlets varies from ten to a few hundred kilometres, the width from a few up to a hundred metres, whereas the depth generally varies from a few to tens of metres. These geometric characteristics are strongly influenced by the tidal climate, possible river inflow and the type of sediment available at that specific site (see Officer 1976). Complex morphodynamic patterns on all length and time scales, such as channel-shoal systems, migrating bedforms (ripples, dunes and sandwaves) and channels, are observed in these tidal embayments. Apart from being morphodynamically active areas in themselves, tidal inlets strongly influence the sediment budget of the coastal system. Furthermore, from an ecological, economical and recreational point of view, these areas usually are very important. Due to this great variety and complexity of tidal inlets and the processes observed in them, as well as the many different fields of interest that can be addressed, various approaches have been used to study tidal inlets (De Vriend 1996). To model and predict the morphological development of tidal inlets, process-based models, i.e. mathematical models based on physical laws, have been developed. These models contain the state-of-the-art physical descriptions and parameterizations. Morphodynamic predictions at time scales shorter than 10 years can be performed. On longer time scales, field observations suggest that there should be certain (empirical) relations between the hydrodynamic forcing and morphodynamic equilibria of tidal inlets. However, such relations cannot be formally derived by analyzing the results obtained with process-based models. It is not even known if a morphodynamic equilibrium exists in

Responsible Editor: Jens Kappenberg

A. Hibma (✉) · H. M. Schuttelaars · Z. B. Wang
Delft University of Technology, PO BOX 5048,
2600 GA Delft, The Netherlands
e-mail: A.Hibma@ct.tudelft.nl

H. M. Schuttelaars
Institute for Marine and Atmospheric research Utrecht,
Utrecht University, Princetonplein 5, 3508 TA Utrecht,
The Netherlands

Z. B. Wang
WL|Delft Hydraulics, P.O. Box 177, 2600 MH Delft,
The Netherlands

the context of a process-based model. This is one of the reasons, maybe even the most important one, why process-based models like Delft3D-MOR cannot be used for long-term morphodynamic simulations in tidal inlets. Another draw-back to these models is that they are too complicated to get more physical insight into which processes are responsible for the observed phenomena. To gain this insight, formally integrated long-term models or idealized models have been developed. These models are also based on first physical principles, but focus on specific morphodynamic phenomena by simplifying the equations in an appropriate way. Due to these simplifications, the results can be analyzed using standard mathematical tools, providing physical insight. Idealized models have proven to be well-suited to study morphodynamic equilibria in tidal inlets (Schuttelaars and De Swart 1996, 2000; Van Leeuwen et al. 2000; Lanzoni and Seminara 2002; Pritchard et al. 2002). However, the influence of the simplifications on the resulting morphodynamic equilibria has never been investigated. Another drawback of these models is that they can only deal with simplified geometries.

In this paper, the idealized model discussed in Schuttelaars and De Swart (2000) and the process-based model Delft3D-MOR described in Roelvink and van Banning (1994) will be used to study the existence of cross-sectionally averaged morphodynamic equilibria for embayments of arbitrary length, forced at the seaward boundary by both a prescribed M_2 and M_4 sea-surface elevation. The focus of this paper is on identifying the main differences between these two models and investigating the influence of these differences on the morphological development. This results, on the one hand, in a justification of the simplifications made in the idealized models. On the other hand, it shows that within the modelling context of the process-based model Delft3D-MOR morphodynamic equilibria exist if the appropriate changes are made to the model formulation. The differences in results of the two models can be related to differences in model formulation and give insight into the importance of these differences on the morphodynamic evolution.

In Section 2 the idealized model and process-based model are shortly discussed. The relevant differences between the two models are identified. The physical formulations in the source code of the process-based model are modified in order to eliminate the major differences between the two models. This results in an intermediate model. In Section 3 the results of the comparison between the idealized and intermediate model will be discussed. It is shown that many results shown in Schuttelaars and De Swart (2000) can be qualitatively reproduced. In Section 4 the influence of the model adaptations on the morphodynamic equilibria will be investigated by removing the adaptations one at a time. In Section 5 the results obtained in the two previous sections will be discussed. In the last section conclusions will be drawn.

2 Description of the models

Previous experiments (Thoolen and Wang 1999) showed that, without adaptations, the idealized and process-based model resulted in different morphodynamic evolution of the basins. This implies that differences between the models concerning the mathematical equations and boundary conditions are essential. Therefore, an intermediate model is developed in which these differences are minimized. The idealized model used in this paper is extensively discussed in Schuttelaars and De Swart (2000) and the process-based model Delft3D-MOR in Roelvink and van Banning (1994) and Wang et al. (1992, 1995). Below we will focus on the differences between the process-based and idealized model and on the resulting intermediate model. In the Appendix a more thorough discussion of the model formulations is given.

The geometry used in all models is that of a rectangular embayment with constant width B (see Fig. 1), i.e. no width variations are taken into account. The side walls of the embayment are non-erodible. The water motion is forced by a prescribed elevation of the free surface η at the entrance of the embayment. River inflow is neglected. The water depth at the landward side of the embayment is assumed to vanish. Due to the surface elevations, the length of the embayment varies in time. The water depth is denoted by D , the water depth at the entrance of the embayment with respect to the mean sea level by H and the horizontal depth-averaged velocity by u .

In all models the water motion is described by the depth-averaged shallow-water equations for a homogeneous fluid. By cross-sectionally averaging the shallow water equations, the width-averaged morphodynamic evolution can be studied. In the idealized model, the bottom friction in the momentum equation is linearized according to the energy dissipation argument discussed in Zimmerman (1992). Furthermore, it is assumed that the ratio of the amplitude of the free surface elevation A and the water depth D is small everywhere in the basin. Near the landward boundary this assumption loses its validity. This will be discussed in more detail in Section 5.

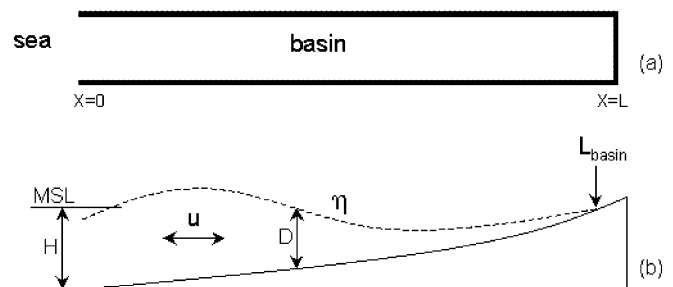


Fig. 1a, b The top view (a) and side view (b) of an idealized geometry as used in the experiments. The symbols are explained in the text. *MSL* denotes the mean sea level

Delft3D-MOR uses a finite difference method to solve the water motion on a staggered grid. Using only one grid cell in the perpendicular direction and applying the zero-flux boundary conditions at the side walls, it is evident that the process-based model effectively solves the cross-sectionally averaged shallow-water equations as well. In the process-based model, a non-linear bottom friction is implemented. The formulation of the bottom friction in the momentum equation is the main difference between the two models concerning hydrodynamics. In the adapted model the linearized bottom friction formulation as discussed in Schuttelaars and De Swart (2002) is implemented. Minor differences between the idealized and intermediate model remain, namely the treatment of the moving boundary at the landward side and the approximations used to prevent the friction term from becoming singular when the water depth vanishes. Furthermore, in the idealized model, it is assumed that the tidal amplitude divided by water depth is always small. Hence, only residual velocities and the M_2 and M_4 tidal constituents are determined, whereas in the process-based model all overtides are taken into account. An overview of the model adaptations and differences is given in Table 1.

The sediment in the embayment is assumed to be uniform and non-cohesive. It is mainly transported as suspended load. In the idealized model this transport is described by a depth-integrated concentration equation. The large shear stresses caused by the tidal currents erode the sediment which gets into suspension. This is parameterized by a sediment pickup function proportional to u^2 . Advective and diffusive processes result in a net transport of sediment which is deposited under the influence of gravity. At the seaward boundary, it is required that, averaged over a tidal period, no net erosion or deposition occurs (i.e. the depth at the entrance is fixed in the idealized model). At the landward boundary, no sediment flux is allowed. In the process-based model the transport of sediment is described by a depth-averaged concentration equation. The pickup function is determined by the suspended transport capacity according to a sediment-transport formula. Depending on the choice of the sediment-transport formula, the effect of the critical velocity for erosion of sediment can

be taken into account. The seaward boundary condition distinguishes between inflow and outflow conditions: during inflow the concentration at the entrance equals the equilibrium concentration, whereas during outflow conditions the concentration is usually calculated dynamically. Contrary to the idealized model, this allows for a change of water depth at the entrance of the embayment. At the landward side, no sediment fluxes are allowed. Bed-load transport is also incorporated in the model, which is neglected in the idealized model. The other main differences between the idealized and process-based model are the parameterization of the erosion of sediment and the boundary condition at the entrance. In the adapted version of Delft3D-MOR, the bed-load transport is set to zero and the sediment pickup function as proposed in the idealized model has been implemented to calculate the equilibrium concentration. At the open sea boundary the dynamic equilibrium sediment concentration is prescribed as a boundary condition. This dynamic equilibrium concentration is determined by solving the local concentration equation in which both the advective and diffusive contributions are neglected. Hence, the variation of the concentration in the water column is determined only by the pickup term and the deposition term. However, this condition does not result in a fixation of the bed at the entrance. The implication of this distinction between the models will be discussed later in Section 4 (exp. 7c, see Table 3). Small discrepancies in the formulation of sediment transport remain between the depth-averaged and depth-integrated model, which are described in more detail in the Appendix. Furthermore, in the idealized model only residual concentrations and the M_2 and M_4 constituents of the concentrations are determined, whereas in the process-based model all constituents are obtained.

In all models, the bed evolution equation is derived from continuity of mass in the sediment layer. Instead of solving this equation dynamically, the solution method in the idealized model tries to find a morphodynamic equilibrium with a prescribed basin depth at the entrance of the embayment and a fixed embayment length. The process-based model tries to find morphodynamic equilibria by time integration. In the original Delft3D-MOR model both the water depth at the entrance and

Table 1 Adaptations in the process-based model formulations and the remaining differences between the intermediate and idealized model

Processes	Adaptation in intermediate model	Remaining different formulation in intermediate model (vs. idealized model)
Hydrodynamics	Linearization of friction term	Drying and flooding procedure Inclusion (vs. neglect of) M_6 and higher overtides
Sediment transport	Calculation of reference concentration Neglect of bed-load transport	Depth-averaged (vs. integrated) concentration Inclusion (vs. neglect of) M_6 and higher constituents in concentration Dynamic concentration at boundary (vs. boundary layer in time-dependent part) Constant (vs. local) depth in equilibrium concentration and time scale
Bed evolution	Fixation of seaward boundary	Variable (vs. constant) embayment length

Table 2 Default model parameters used in the experiments

Parameter	Definition	Default value
H	Depth at entrance	10 m
$A_{M_2(x=0)}$	Tidal amplitude	1.75 m
$\phi_{\eta, M_2(x=0)}$	Phase difference	0 rad
C	Chézy coefficient	$70 \text{ m}^{1/2} \text{ s}^{-1}$
ρ_s	Mass density of sediment	2650 kg m^{-3}
d_{50}	Grain size	200 μm
w_s	Fall velocity susp. sed.	0.033 m s^{-1}
ϵ_x	Dispersion coefficient	$10 \text{ m}^2 \text{ s}^{-1}$
γ	Deposition coefficient	$4 \times 10^{-3} \text{ s}^{-1}$
α_e	Pickup coefficient	$3 \times 10^{-2} \text{ kg s m}^{-4}$
U_r	Characteristic velocity	1 m s^{-1}
σ	Tidal frequency	$1.4 \times 10^{-4} \text{ s}^{-1}$

Table 3 Model experiments with intermediate model

Exp.	Simulation with intermediate model	Figure
1	Simulation of hydrodynamics on equilibrium profiles found with idealized model for embayments of 50, 100 and 150 km lengths forced with M_2 tide	Figs. 3, 4, 5
2	Simulation of hydrodynamics on deep and shallow profile for an embayment length of 145 km, which form multiple equilibria in idealized model forced with M_2 and M_4 overtide	Figs. 7, 8
3	Morphodynamic simulations during 750 years starting from the equilibrium profiles of the idealized model	Fig. 9a, c
4	Morphodynamic simulations during 750 years starting from a linear sloping profile	Fig. 9b, d
5	Morphodynamic simulations starting from multiple equilibrium profiles of idealized model	Figs. 10, 11
6	Morphodynamic simulations starting from manually adapted deep profile	Fig. 16
7	Morphodynamic simulations during 300 years starting from linear profile, where model adaptations in intermediate model are replaced by formulations used in Delft3D-MOR	Figs. 12, 13, 14

the length of the embayment are allowed to change. In the intermediate model the bed evolution is solved by requiring the bed to be fixed at the entrance. Hence, only the length of the embayment is variable due to sedimentation erosion at the landward end.

3 Model results

In this section it will be shown that with the intermediate model, the main characteristics of the morphodynamic equilibria obtained with the idealized model and their dependency on parameters can be reproduced. In Section 3.1 the water motion resulting from the intermediate and idealized model will be compared. Using the equilibrium bed profiles obtained with the idealized model, the water motion is calculated with the intermediate model and compared with the water motion given by the idealized model. In these experiments the length of the embayment and the forcing at the entrance will be varied. The default parameters are shown in Table 2 and the experiments are listed in Table 3.

In Section 3.2 the morphodynamic evolution of bed profiles towards equilibrium in the intermediate model will be discussed and compared with the evolution resulting from the idealized model. Both the influence of embayment length and external forcing will be investigated. Furthermore, the choice of the initial bed and the adaptation towards equilibrium will be discussed.

3.1 Hydrodynamic results

In Schuttelaars and De Swart (2000) it is shown that a unique morphodynamic equilibrium exists for all embayment lengths L shorter than the M_2 frictional length scale of the tide, if the system is forced only by a prescribed M_2 tide at the seaward boundary. In Fig. 2 the equilibrium bed profiles from the idealized model for basin lengths of 50, 100 and 150 km are shown. The horizontal velocity fields resulting from the intermediate and idealized model are compared for these basins (exp. 1, see Table 3). To make a good comparison possible, the horizontal velocity is decomposed in its tidal components:

$$u = \langle U \rangle + U_{M_2} \cos(t - \phi_{M_2}) + U_{M_4} \cos(t - \phi_{M_4})$$

with $\langle U \rangle$ the residual velocity. Here U_{M_2} and U_{M_4} denote the amplitudes of the horizontal velocity components of

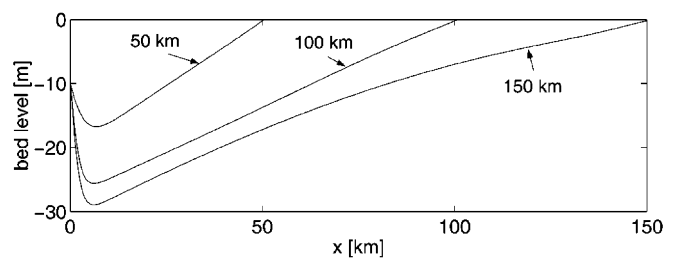
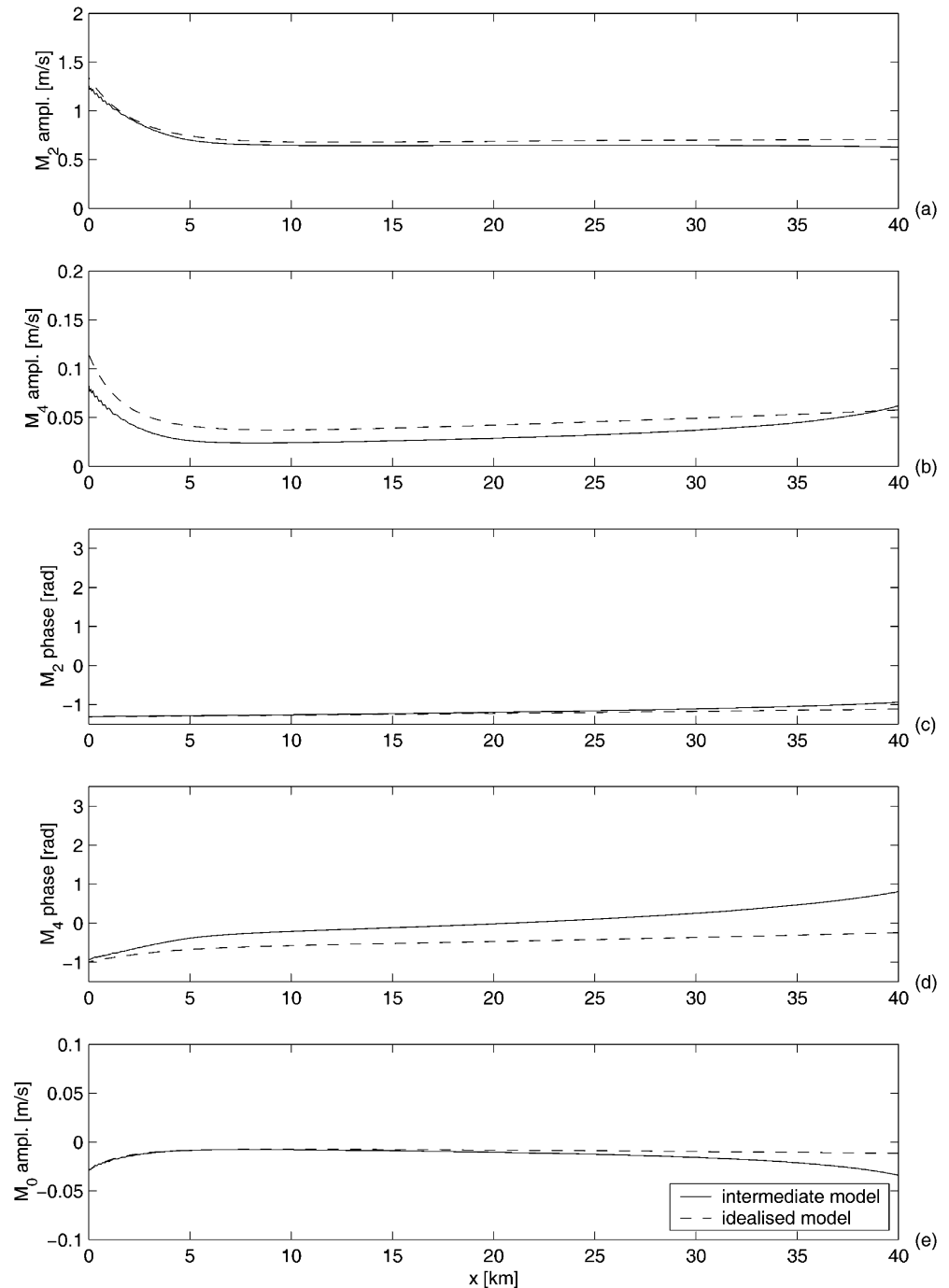


Fig. 2 Equilibrium bed profiles for embayments of 50, 100 and 150 km length. The parameter values are given in Table 2

the M_2 and M_4 tidal constituents, respectively, and ϕ_{M_2} , ϕ_{M_4} their respective phases. Since in the idealized model other tidal components are neglected, these components are not determined for the velocity field obtained by the intermediate model. Due to the flooding and drying of the basin in the intermediate model at the landward side, it is not possible to make an accurate tidal decomposition in this region. Therefore, only amplitudes and phases obtained in that part of the embayment that is not subject to flooding and drying in the intermediate model are compared to the results found in the idealized model.

For basin lengths much shorter than the tidal wave length, a standing wave is observed in the idealized model. The basin of 50 km length can still be considered short compared to the tidal wave length. For this basin the amplitudes of the M_2 and M_4 tidal velocities are shown in Fig. 3a and b, their phases in Fig. 3c and d and the residual component in Fig. 3e. The correspondence between the models concerning the M_2 tidal component, both the amplitude and the phase, is excellent. Clearly, the standing wave character of the water motion is recovered by the intermediate model. Concerning the M_4 tide and the residual velocity, the similarities are still

Fig. 3a–e The tidal constituents of the horizontal velocity fields resulting from the idealized (*dashed line*) and intermediate model (*solid line*) for an embayment with a length of 50 km. Other parameter values are as given in Table 2. The M_2 amplitude is shown in **a**, M_4 amplitude in **b**, the M_2 phase, M_4 phase and the residual velocity in **c**, **d** and **e**, respectively (exp. 1a, see Table 3)

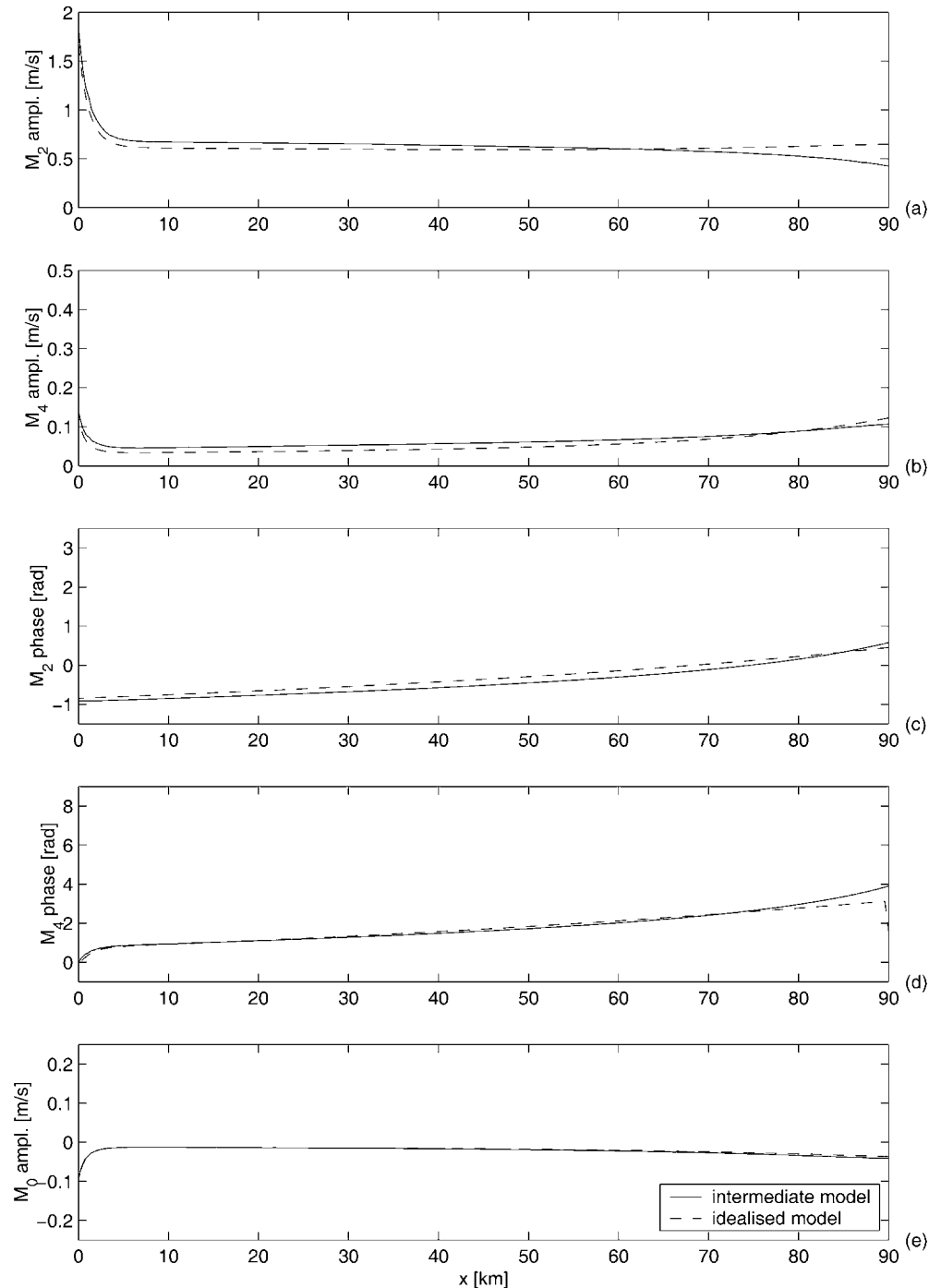


very good close to the entrance of the embayment. Moving towards the landward side of the embayment, the solutions from the idealized and intermediate model start to deviate. This is probably due to the differences in model formulations for small depths, as will be discussed in Section 5.

If the length of the embayment is increased, the embayment will become resonant. According to the idealized model, this will occur for embayment lengths of the order of a 100 km. For longer embayments, the horizontal velocities at the entrance will decrease again.

This result of the idealized model is observed in the intermediate model as well. Comparing the M_2 amplitude at the entrance of the embayment for a 100- and 150-km-long embayment, a decrease of amplitude is observed (see Figs. 4a and 5a, respectively). Near resonance, the tidal wave still has a standing character (Fig. 4c), whereas for embayments much longer than the resonance length a tidal wave with a travelling character is found (Fig. 5c). Again, the main deviations between the model results are found in the M_4 tides and the residual velocities near the end of the embayment.

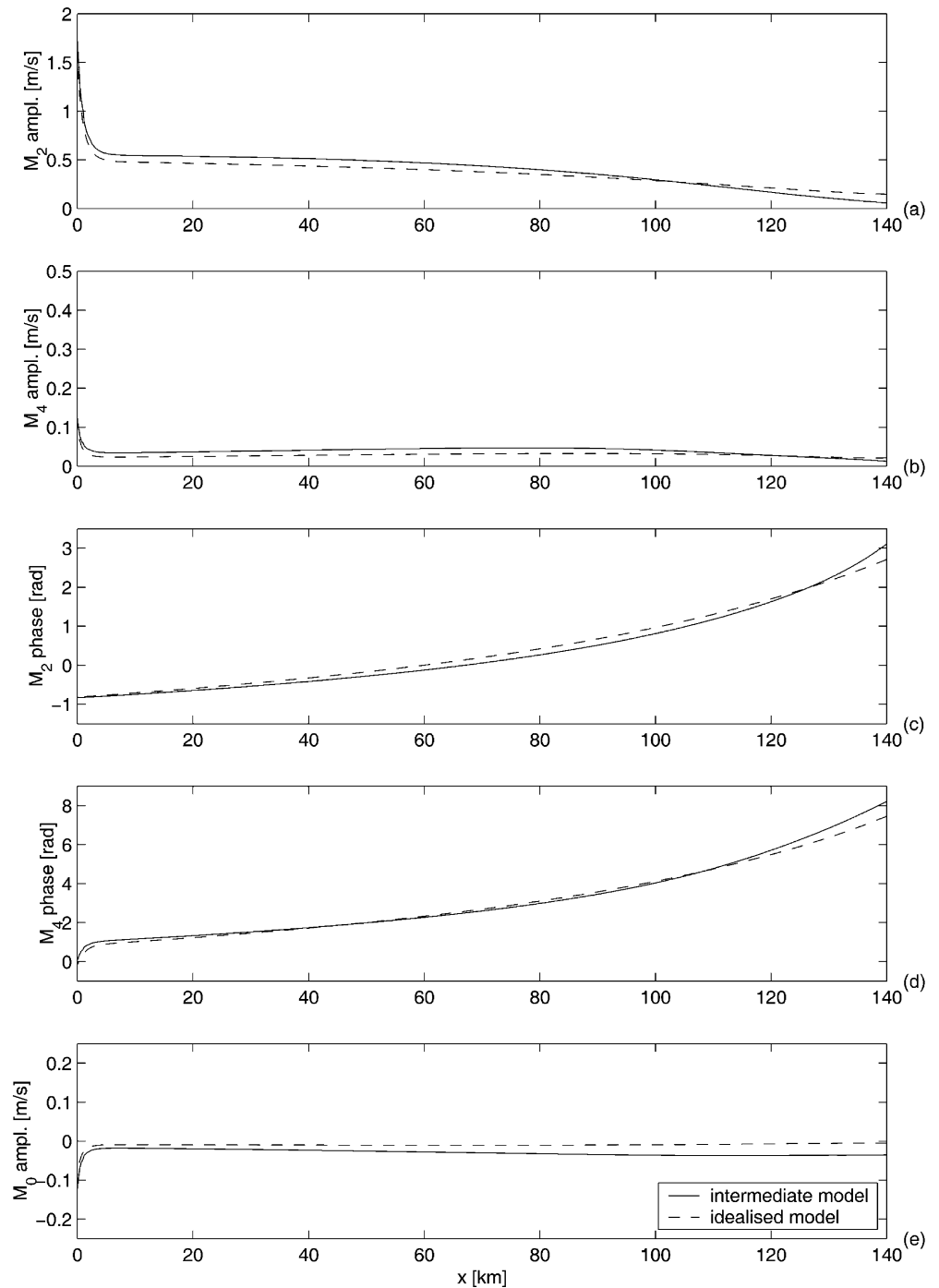
Fig. 4 As Fig. 3, but using an embayment length of 100 km (exp. 1b)



If an externally prescribed overtide is imposed as well, different types of equilibria are found in the idealized model. For L values smaller than the M_4 resonance length, the bottom profiles are strongly concave, with locally large water depths. The water motion resembles a standing tidal wave. For longer embayments, another type of equilibria, characterized by a weakly concave bottom profile and a travelling tidal wave, appears. For sufficiently strong amplitudes of the externally prescribed M_4 tide, multiple morphodynamic equilibria are found, having the different character

described above. Therefore, an embayment length and forcing are chosen in such a way that both types of morphodynamic equilibria occur for the same embayment length. An example is shown in Fig. 6 for an embayment with a length of 145 km. The amplitude of the M_2 sea-surface elevation at the entrance is 1 m and of the M_4 sea-surface elevation is 0.074 m. The relative phase between the M_2 and M_4 tidal components is 0° . The depth at the entrance is $H = 15$ m. Other parameters are as defined in Table 2. The horizontal water motion corresponding to the deep bed profile is shown in

Fig. 5 As Fig. 3, but using an embayment length of 150 km (exp. 1c)



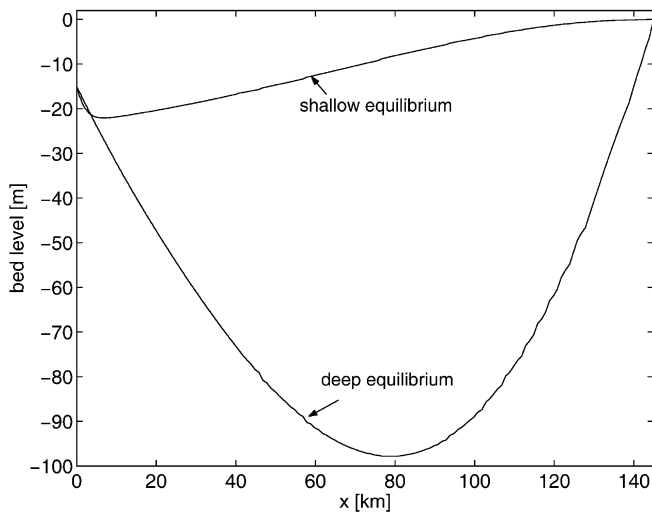


Fig. 6 The two stable equilibrium bed profiles for an embayment with a length of 145 km, resulting from the idealized model. The system is forced by both a prescribed M_2 and M_4 tidal elevation at the entrance [$A_{M_2}(x=0) = 1$ m, $A_{M_4}(x=0) = 0.074$ m, and both phases 0 rad]. The other parameter values are given in Table 2

Fig. 7 (exp. 2). The amplitude of the M_2 tidal component shows good agreement throughout the complete basin. The comparison between the amplitudes of the M_4 tidal component and the residual current is quite satisfactory near the end of the embayment. However, at the entrance, considerable differences are observed. In both the idealized and intermediate model results, no spatial dependency in the phases of the M_2 and M_4 phases is observed, hence a standing wave solution is found. Although the M_2 phases in both models are almost identical, a large difference is observed between the M_4 phases. This is due to the combination of the internally generated and externally prescribed M_4 phases, as will be discussed in more detail in Section 5.

For the shallow bed profile, Fig. 8 shows that the water motion found by the two models compares quite well near the entrance of the embayment. However, near the landward side of the embayment, the correspondence becomes much poorer.

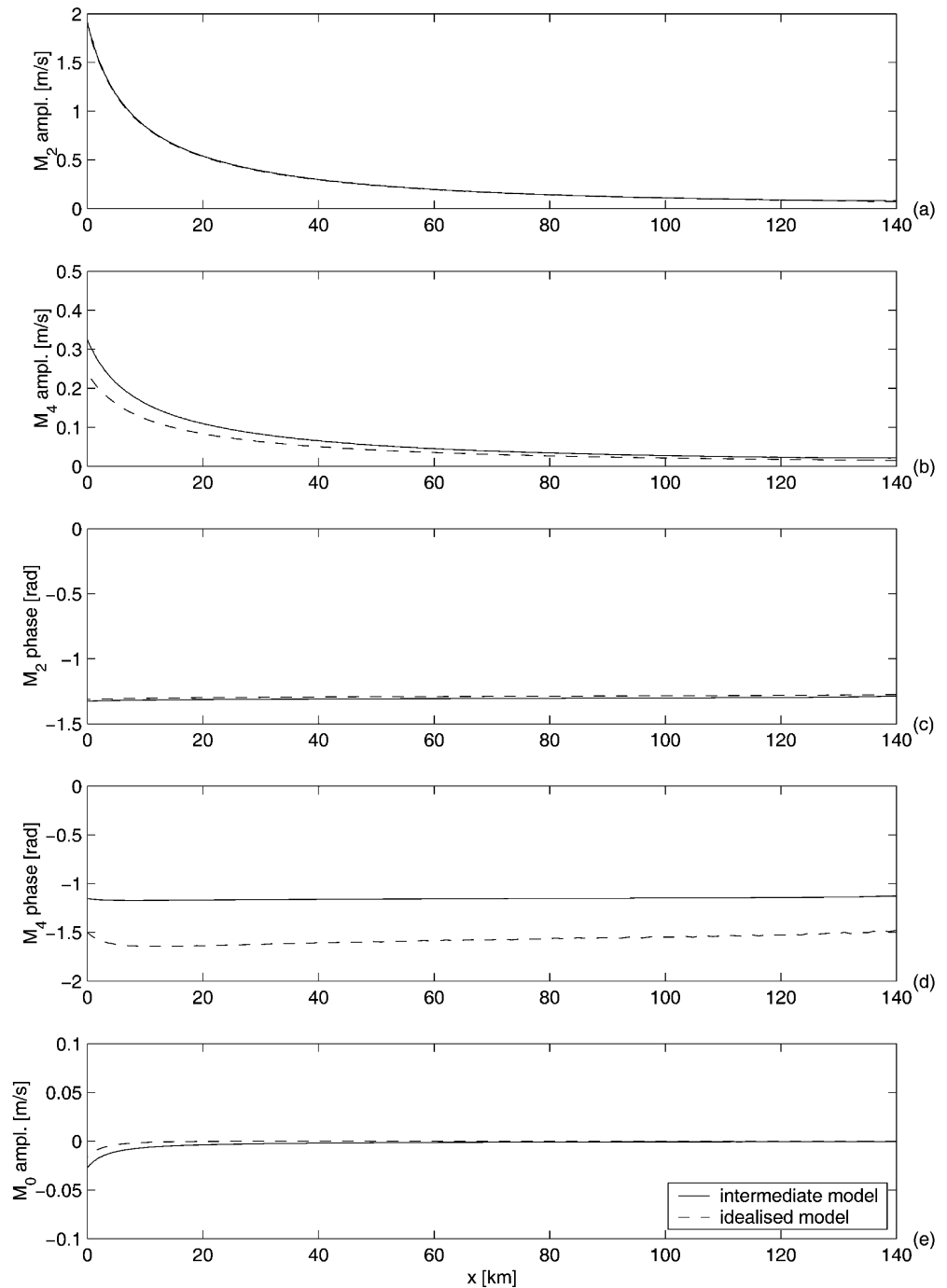
3.2 Morphodynamic results

In Fig. 2 the equilibrium bed profiles as found in the idealized model are shown for basin lengths of 50, 100 and 150 km. The basin was forced only by an M_2 sea-surface elevation at the seaward boundary. According to Schuttelaars and De Swart (2000), the morphodynamic equilibrium is unique and stable. This implies that any arbitrary initial profile should evolve towards this equilibrium. In the first morphodynamic experiment, the bed profiles found in the idealized model will be used as initial bed profiles (exp. 3). The bed profiles after 750 years are shown in Fig. 9a. These profiles qualitatively resemble the equilibrium profiles from the idealized

model: a deep pool is found near the entrance of the basin, whereas the bed is more or less constantly sloping with a zero depth at the landward side. During the first years of evolution, relatively large changes are observed near the entrance of the embayment. The deep pool, as observed in the results of the idealized model, starts to fill up. The adjacent profile also shallows in landward direction. For the basin lengths of 100 and 150 km this process is not completed after 750 years, which causes the hump around $x = 25$ km in the profiles. As can be inferred from Fig. 9c, the time needed to evolve towards the new equilibrium depends on the embayment length. In this figure, the yearly change in bed height averaged over the complete basin length is shown as a function of time. For an inlet of 50 km, Fig. 9c shows that after approximately 40 years the changes to the bed are negligible compared to the initial changes. Continuing the time-integration leads to sedimentation at the landward side of the embayment and hence a shortening of the embayment. For longer embayments, the same evolution can be observed. However, the corresponding initial phase of relatively fast adaptation is much longer. To make the uniqueness of the morphodynamic equilibrium plausible, another initial bed profile is chosen for all embayment lengths. This bed is chosen to be constantly sloping (exp. 4, see Fig. 9b). Again, the same observations concerning the evolution can be made. The initial evolution is (relatively) fast, but in this case a pool is being formed near the entrance. After some time (in this case approximately 200 years) the amplitude of the bed changes integrated over the basin decreases exponentially. Again, the quasi-equilibrium profiles found in the intermediate model show a good qualitative agreement with the equilibrium profiles predicted by the idealized model. Although these bed changes do not go to zero, even after integrating for a long time (here 750 years), they become very small and affect mainly the length of the basin. This adaptation of the length also prevents a quantitative agreement between the developed profiles starting from the different initial profiles, because the lengths of the basins no longer coincide.

Previous results show that morphodynamic equilibria exist in the intermediate model. As already discussed, the idealized model predicts the existence of multiple equilibria for a basin length of 145 km and $A_{M_2}(x=0) = 1$ m, $A_{M_4}(x=0) = 0.074$ m and $\phi_{\eta, M_2}(x=0) = \phi_{\eta, M_4}(x=0) = 0$ rad (see Fig. 6). Using these equilibria as initial profiles, their morphodynamic evolution can be studied (exp. 5). The equilibrium with the relatively shallow bed has the same morphodynamic evolution as those forced only with an M_2 tidal component (see Figs. 10 and 11a): in the first few decades, a relatively fast bottom change takes place near the entrance of the embayment and the pools become less pronounced. Next, the basin slowly starts to fill up at the end. Due to this adaptation of the basin length, the profile starts to deepen again near the entrance of the basin. The evolution of the basin, starting from the other equilibrium, shows that a lot of deposition takes place in the

Fig. 7a–e The tidal constituents of the horizontal velocity fields resulting from the idealized (*dashed line*) and intermediate model (*solid line*) for an embayment length of 145 km, being forced by both an M_2 and M_4 tidal component at the entrance of the embayment. The equilibrium bed used in this experiment is the deep profile shown in Fig. 6. Other parameter values are given in Table 2. The M_2 amplitude is shown in **a**, M_4 amplitude in **b**, the M_2 phase, M_4 phase and the residual velocity in **c**, **d** and **e**, respectively (exp. 2a)



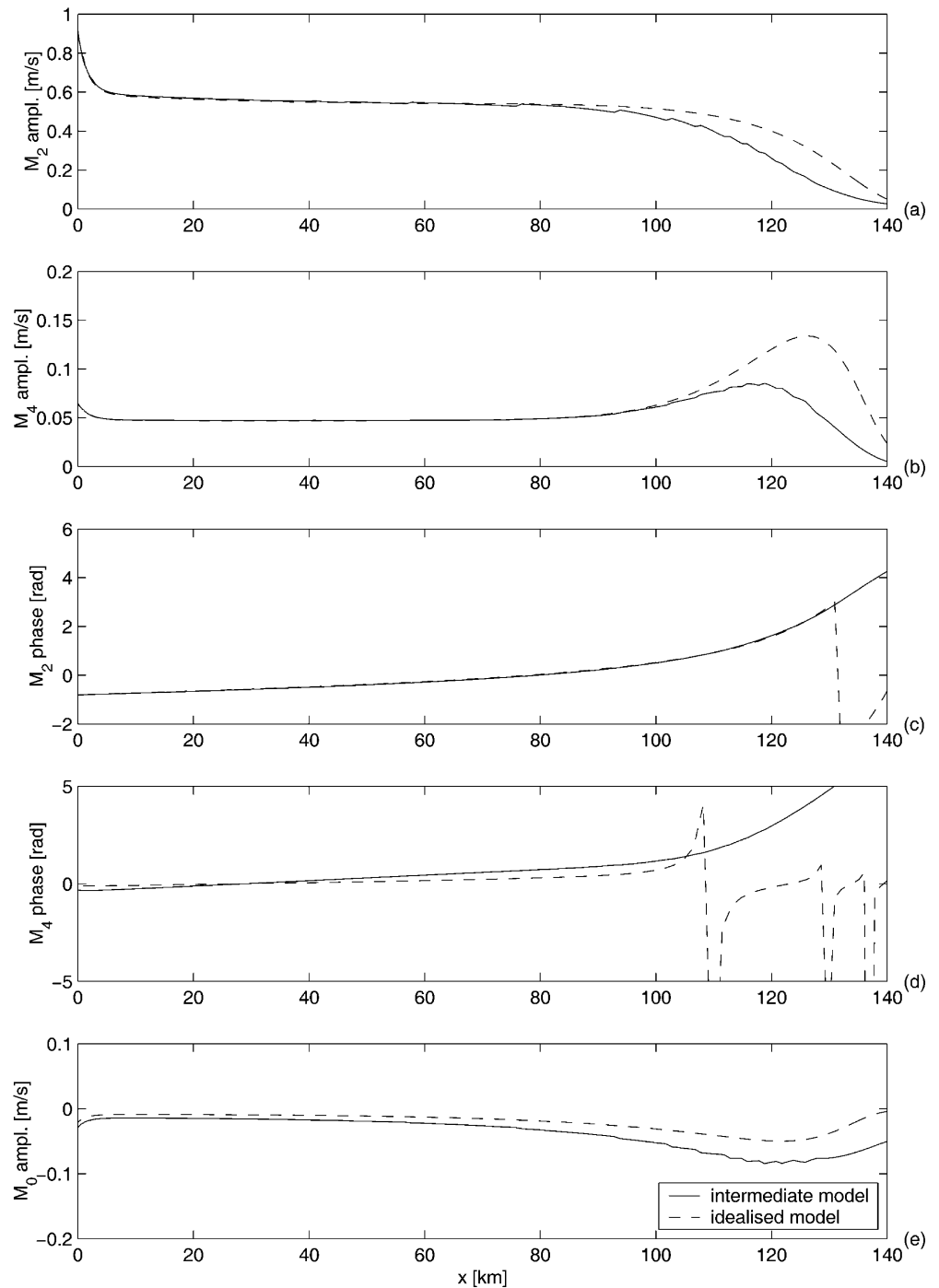
embayment (see Figs. 10 and 11b). The embayment is filling up, starting near the entrance, just as in the case of a shallow equilibrium bed. After approximately 10 000 years, the erosion deposition in the first 40 km of the embayment becomes negligible. Moving from this region of no erosion deposition, a very active morphodynamic region is found. Here, large amounts of sediment are still deposited. Moving even further towards the end of the embayment, again no morphodynamic activity is observed. This region of morphodynamic activity is slowly moving towards the end of the embayment. In Section 5

it will be discussed if this profile can be regarded as a second equilibrium in the intermediate model.

4 Influence of model differences

In the previous section it was shown that the main characteristics of the morphodynamic equilibria found in the idealized model could be reproduced by the intermediate model. In this section, the effects of the adaptations in the process-based model (i.e. the main

Fig. 8 As Fig. 7, but now with the shallow equilibrium bed (exp. 2b)



model differences between the idealized and process-based model) on the morphodynamic evolution of the basin will be discussed. To this end, the changes made in the source code of Delft3D-MOR will be removed one at a time. This results in a number of adapted models. In each adapted model, one difference is removed, the other adaptations remain as in the intermediate model. For every adapted model, a time integration will be performed for a basin of 50 km over a period of 300 years (exp. 7). The initial bed is constantly sloping. These

results will be compared with those resulting from a time-integration done with the intermediate model. The differences between the results is a measure for the importance of these model adaptations with respect to the morphodynamic evolution. This analysis will clearly pinpoint the reason for the different model results between the idealized and process-based model as reported in Thoolen and Wang (1999).

The first major difference between the intermediate model and the process-based model is the formulation



Fig. 9. a–d Top figures The bed profiles after 750 years of evolution (solid line) of tidal embayments with lengths of 50, 100 and 150 km, starting from the equilibrium bed profiles as obtained in the idealized model (dashed line, a) and constantly sloping initial bed (dashed line, b). Parameter values are given in Table 2. In the lower figures the bed change, averaged over the basin, in m a^{-1} , is shown as a function of time. Note that negative (positive) values denote a decrease (increase) of water depth (a and c from exp. 3; b and d from exp. 4)

of the bottom friction. In the intermediate model the friction is linearized. In the adapted model the original non-linear bottom friction description is reintroduced. Initially, it results in increased velocities, accompanied by larger sediment transports. However, this does not lead to distinct differences in the profiles at the end of the simulation period, see Fig. 12.

Two adaptations were made in the transport formulation: neglecting the bed-load transport and the implementation of the sediment pickup function. First, these adaptations are separately removed. The bed-load transport appears to contribute little to the total amount of transported sediment. The use of a different sediment pickup function (the adaptation in the suspended sedi-

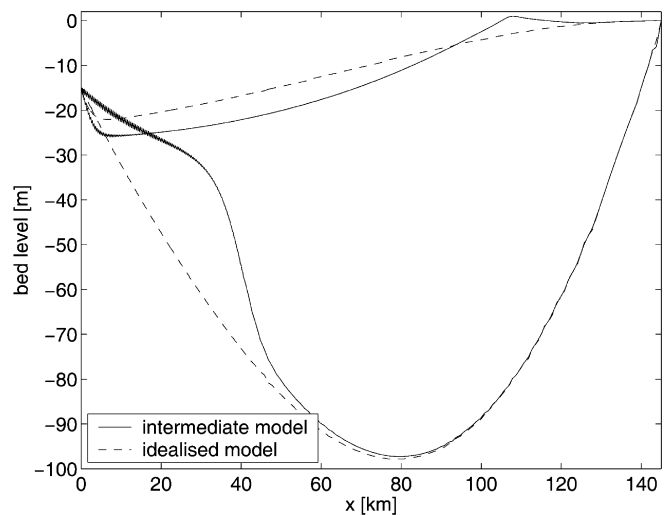


Fig. 10 The bed profiles (solidlines) for an embayment length of 145 km found after a time integration of 10 000 years with initial profiles denoted by the dashed lines. The system is forced by both an M_2 and M_4 tidal component at the entrance of the embayment. Other parameter values are given in Table 2 (exp. 5)

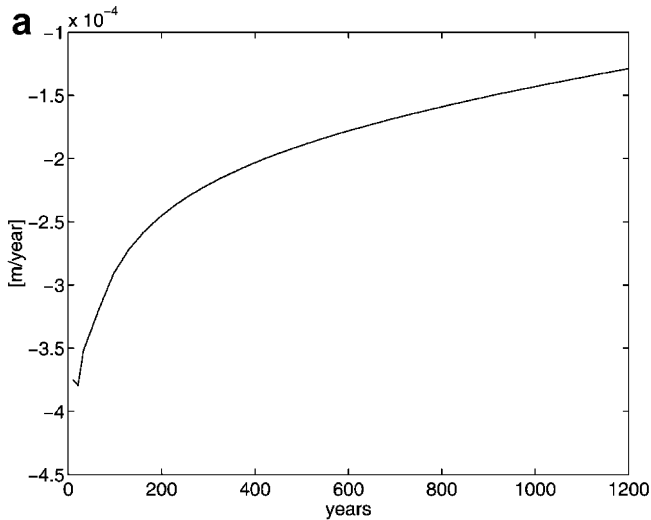
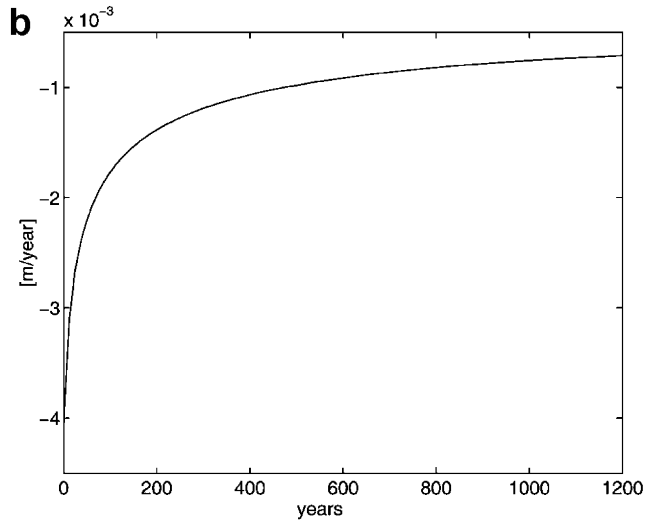


Fig. 11 Here the bed changes, averaged over the basin, in m a^{-1} , are shown as a function of time. Note that *negative (positive) values* denote a decrease (increase) of water depth (exp. 5)

ment formulation) mainly effects the time scale of the development of the profile. This time scale is sensitive to the choice of the sediment pickup and erosion coefficients. Besides this, a slightly steeper slope is found applying the adapted formulation, which can be the result of relatively stronger erosion near the entrance induced by the adapted formulation for the equilibrium concentration. In Fig. 13 the resulting bed profile after 300 years is shown when all adaptations to the sediment transport formulations are removed.

Contrary to the previous model adaptations, the description of the boundary condition at the entrance of the embayment has qualitative influence on the morphodynamic evolution of the embayment. In the



intermediate model the bottom level at the entrance is fixed independently of the sediment- transport direction, whereas in the Delft3D-MOR description the bottom level is fixed only if the residual sediment transport is inwards (see Wang 1992 and Appendix). This difference results in a continuing deepening of the profile during the simulation (see Fig. 14). In Section 5 this modelling aspect is discussed in more detail.

5 Discussion

5.1 Hydrodynamics

In the previous sections the comparison of the intermediate and idealized model results and the effects of the model adaptations in the process-based model were shown. In this section these results will be discussed and

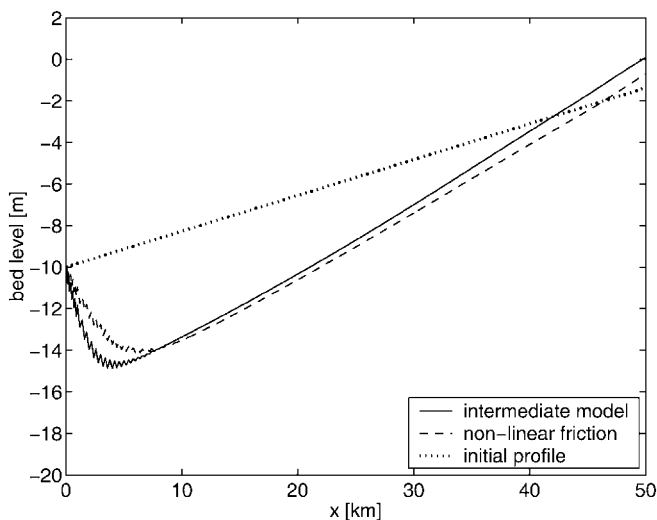


Fig. 12 Longitudinal profile after 300 years, starting from a linear slope, applying linearized friction (*solid*) and non-linear friction (*dashed*) (exp. 7a)

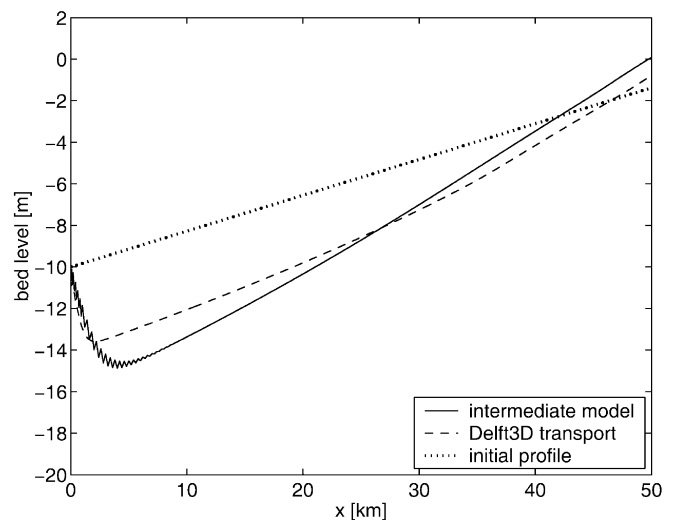


Fig. 13 Longitudinal profile after 300 years, starting from a linear slope, applying adapted transport formulations (*solid*) and Delft3D-MOR formulations (*dashed*) (exp. 7b)

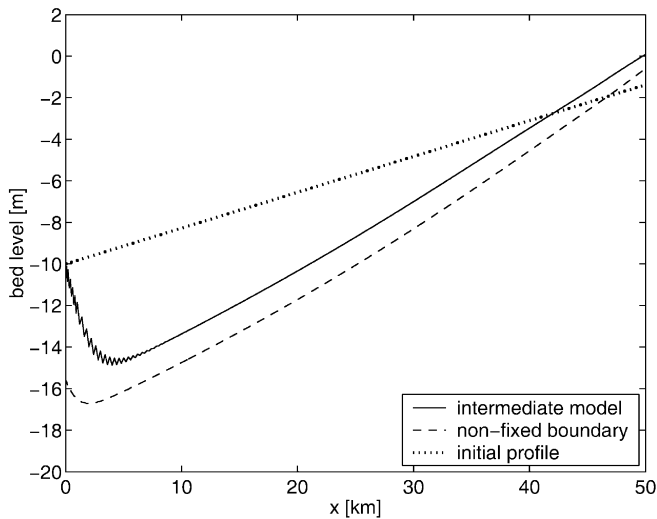


Fig. 14 Longitudinal profile after 300 years, starting from a linear slope, applying a fixed boundary (*solid*) and Delft3D-MOR formulations (*dashed*) (exp. 7c)

the differences and consequences of the adaptations to the process-based model will be explained.

Both a qualitatively and quantitatively good agreement between the hydrodynamics of the intermediate and idealized model is found. When forcing the system only with a prescribed M_2 sea-surface elevation, the characters of the tidal wave and its dependence on the basin length are recovered by the intermediate model. Maximum velocities are observed in the basin, which has approximately the resonance length. A standing wave occurs in relatively short and a travelling wave in long embayments. Small differences are observed, mainly in M_4 tides and the residual current near the end of the embayment. These deviations are the result of two remaining differences in the water motion description. One is the neglect of the M_6 tide and higher overtides in the idealized model. Additional analysis of the water motion showed that these components are one order of magnitude smaller than the M_4 component and therefore not expected to cause the main deviations. The other difference is the treatment of the moving landward boundary. In the idealized model formulation, it is assumed that the sea-surface elevation is always much smaller than the undisturbed water depth, i.e. the distance from the bed to the mean sea level. This is, of course, no longer valid near the landward side of the inlet. In the intermediate model, this assumption is not made. The flooding and drying of shallow parts is represented by removing grid cells, that become dry when the tide falls, and reactivating cells, that become wet when the tide rises. This difference in model formulation occurring for the shallow landward part also influences the water motion in the rest over the basin and is most likely to cause the differences in model results.

When the system is forced by an external overtide as well, the model results do not compare as well as in the

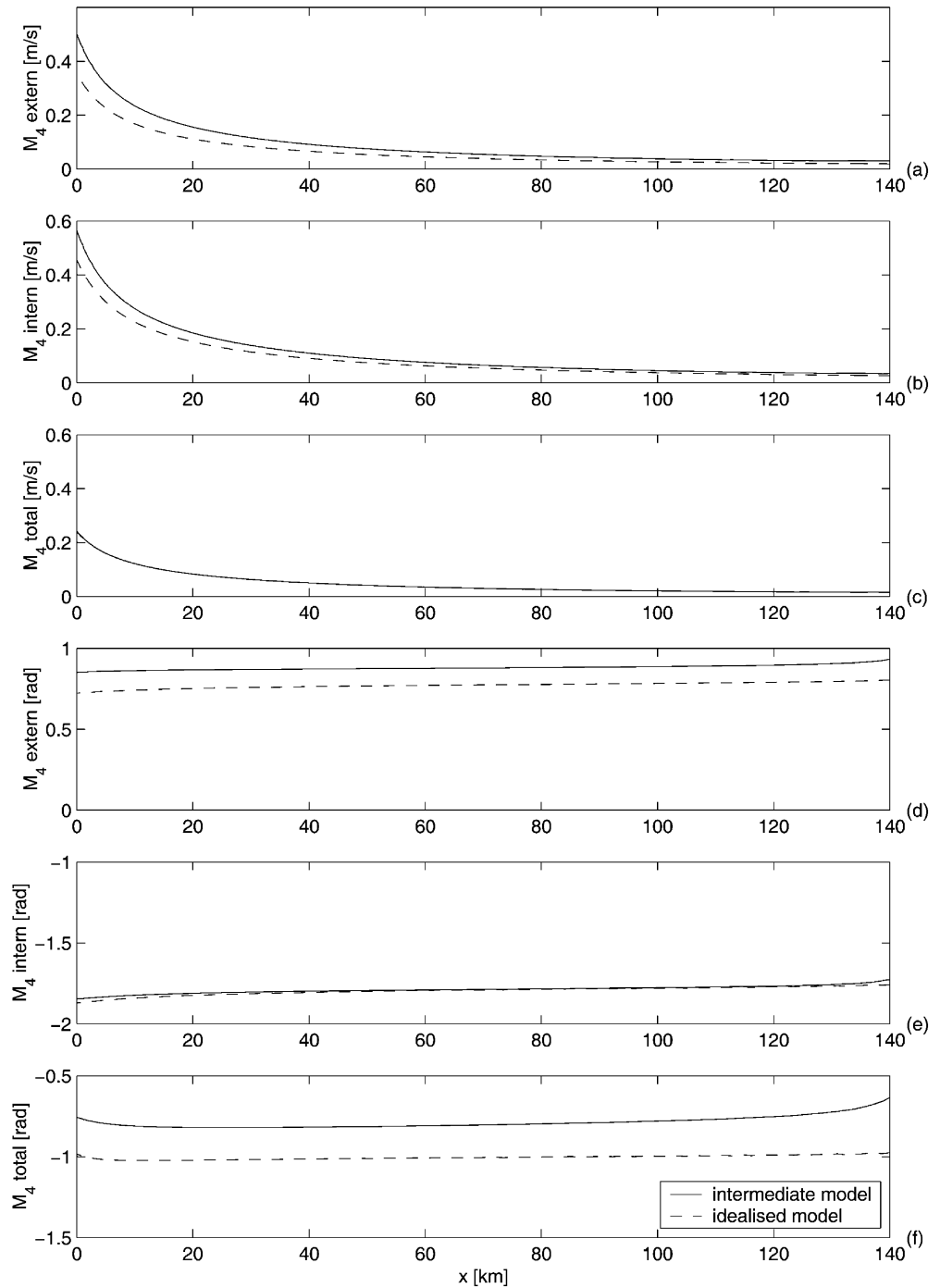
case with only an M_2 forcing. Although the M_2 component of the water motion shows good agreement, both qualitatively and quantitatively, a large difference in the M_4 amplitude and phase is observed. To investigate this further, a decomposition is made between the internally generated M_4 tide, resulting from non-linear interactions between the M_2 components, and the externally forced M_4 component. In the intermediate model this decomposition is approximated by forcing the embayment with only a prescribed M_2 or M_4 sea-surface elevation. Figure 15 shows that both the internal and external M_4 amplitudes and phases as found in the models agree quite well, showing differences smaller than $0.2 \text{ m}^3 \text{ s}^{-1}$ and 0.2 rad , respectively. Combining the internal and external components, the small differences in amplitude and phase result in larger deviations of $0.2\text{--}0.3 \text{ rad}$ in the combined M_4 phase, though a negligible deviation in the combined M_4 velocity (see Fig. 15f and c, respectively).

5.2 Morphodynamics

Differences in the velocity field, albeit small, imply that the sediment transport field and therefore the morphological equilibria deviate. The morphological development of the longitudinal profiles forced by the M_2 show only initially the largest changes near the entrance of the embayment, after which the adjustments rapidly decrease. These initial changes are due to the remaining difference in the sediment-transport formulation. However, qualitatively the resulting profiles resemble the equilibrium profiles of the idealized model. Therefore, the processes found in this model can be adopted for the intermediate model, which is a balance between sediment fluxes resulting from the interaction of the main M_2 tide and internally generated overtides in velocity and concentrations. An equilibrium is not achieved in the intermediate model in the strict sense of zero net sediment transport throughout the basin. In Schuttelaars and De Swart (1996, 2000) it was shown that to reach an equilibrium in the strict sense, it is essential that a finite velocity is allowed at places where the depth vanishes (i.e. only the water flux has to become zero at these points). This condition is not implemented in the intermediate model. Therefore, an equilibrium in the strict sense will never be found. Due to the sedimentation, the length of the basin decreases. For this new basin length the profile is no longer an equilibrium. This again results in morphodynamic changes, which are most pronounced at the entrance of the basin. Theoretically, it can be expected that this process will eventually lead to a trivial equilibrium, i.e. the complete filling up of the basin. A possible solution to avoid this behaviour could be the implementation of a (small) river flow at the landward end, thereby allowing a finite velocity at the landward side.

Prescribing an overtide, multiple equilibria were found in the idealized model for certain basin lengths. The morphodynamic evolution starting from the multi-

Fig. 15 a–f In this figure, the M_4 amplitude and phase as shown in Fig. 7 are decomposed in the amplitude (**a** and **b**) and phase (**d** and **e**) of the externally forced and internally generated components, respectively. In **c** and **f** the internally generated and externally forced M_4 velocities and phases are added (exp. 2c)



ple equilibrium is simulated for a long period in the intermediate model. In the idealized model the shallow basin shows a type of evolution similar to those without an externally prescribed overtide. This can be understood by realizing that for this equilibrium a balance is found between sediment fluxes resulting from the interaction of the main M_2 tide and internally generated overtides only. The externally generated velocities are too weak to contribute substantially to this balance. On first sight, the evolution of the deep basin looks com-

pletely different. However, the qualitative changes near the entrance are identical to those shown in, for example Fig. 9a where the embayment is forced only by a prescribed M_2 tide: the embayment starts to become shallower due to the difference in the sediment-transport formulation. The deposition term in the intermediate model is not dependent on the local depth as in the idealized model, which results in much larger deposition for the large depths in this basin. This process is slowly moving from the entrance of the embayment to the

landward side. Due to the large depth, the changes in this case are larger than in Fig. 9a. However, the standing tidal wave is maintained during this evolution and the presence of the externally forced overtide remains important. The sediment fluxes resulting from the interaction between the main M_2 tide and these externally prescribed overtides balance those from the interaction between the main M_2 tide and the internally generated overtides, hence this equilibrium (see Fig. 10) is a completely different morphodynamic equilibrium as compared to the one observed using a shallow initial bed.

To investigate if this balance remains different when the trend of deposition near the entrance is continued, the profile is adapted manually using the information of the first 10 000 years (i.e. the tendency to filling observed in Fig. 10 is continued). This profile is used as initial profile for morphodynamic computations during another 10 000 years. Figure 16 shows that on this profile, the main changes do not occur near the entrance, but in the middle and landward part of the basin, where deposition is observed. For this long simulation period the changes look considerable. However, note that 10 000 years is simulated versus 750 years in expts. 3 and 4. The yearly adaptation rate is of the same order of magnitude as those at the end of the simulation periods observed in Figs. 9 and 11a. These rates are negligible compared to the initial changes, and mainly contribute to the process of shortening of the basin, which was found to prevent the existence of equilibria in the intermediate model in the strict sense of zero net transport. The shape of the profile remains qualitatively different from the shallow basin during the simulation period, as the deepest part is located more landward. Finally, the tidal wave in this basin has preserved its

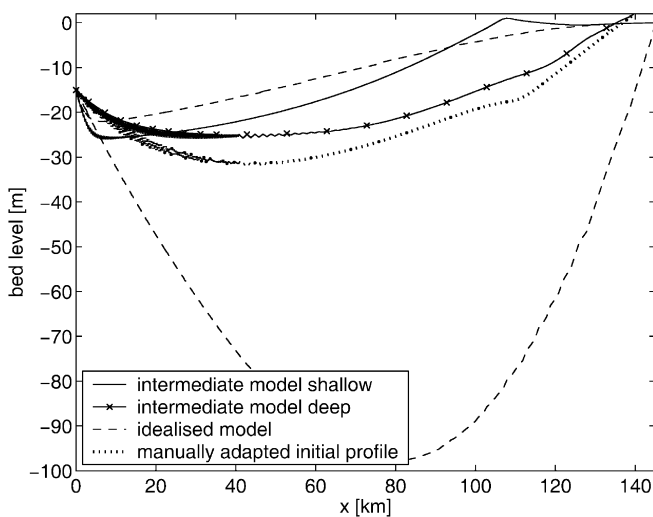


Fig. 16 The bed profile (*crossed line*) for an embayment length of 145 km found after a time integration of 10 000 years with the manually adapted initial profile denoted by the *dotted line*. The system is forced by both a prescribed M_2 and M_4 tidal elevation at the entrance [$A_{M_2}(x=0) = 1$ m, $A_{M_4}(x=0) = 0.074$ m, and both phases 0 rad]. The other parameter values are given in Table 2 (exp. 6)

standing character, which indicates that the balance between the fluxes still differs from those in the shallow basin. Hence, apart from the ongoing shortening process, multiple equilibria due to an overtide exist in the intermediate model, resembling the multiple equilibria of the idealized model.

5.3 Model differences: boundary condition

In the last step of this study, the main differences between the idealized and process-based model were investigated by removing the model adaptations. No qualitative influence on the model results was found for the simplifications made in the hydrodynamic and sediment-transport formulations. Thus, the influence of the linearization of the friction term on the morphological development is shown to be small, as well as the neglect of bed-load transport and the use of a simplified sediment pickup function. Only the fixation of the seaward boundary is found to have qualitative influence. When the bed at this point is allowed to change according to the Delft3D-MOR description, a deepening of the bed is observed during the simulation. This can be explained as follows: in the basin, the bed evolution in Delft3D-MOR depends on the gradients in the sediment transport of the transport field at each time step. At the boundary the procedure slightly differs. At this point the tidally averaged transport is used to determine the bed evolution. If this net transport is directed into the estuary, an extra boundary condition has to be prescribed, which is the fixation of this point. If the tidally averaged transport is directed outwards, the gradients in this transport determine the evolution of this point, resulting in an increase or decrease of the depth. From the development observed in the simulation, it is expected that the deepening will continue until the velocity has decreased below the critical velocity for erosion. Thus, no equilibrium depth exists if the critical velocity is zero. The other option, sedimentation at the boundary, can lead to another trivial profile, i.e. the closure of the basin due to continuous filling of the basin.

Fixation of the boundary during inward- and outward-directed transport as applied in the idealized model prevents the development of these trivial solutions. However, the profile is also not realistic near the entrance, showing a steep slope into a deep pool.

Since the boundary condition at the entrance used in both the idealized and process-based model of the basin can be disputed and no boundary condition is accepted as the correct one in literature, it is recommended to circumvent this difficulty by extending the model region to include (at least) the ebb-tidal delta.

6 Conclusion

The results of the idealized and intermediate model show good agreement with respect to the water levels and

velocities in a schematized estuary. The development of the cross-sectionally averaged profiles in the process-based model resemble qualitatively the unique and multiple equilibrium profiles of the idealized model, although an equilibrium is not achieved in the strict sense of zero net sediment transport.

Using the idealized model, the physical processes resulting in the equilibria are identified: when no overtide is prescribed, the balance between sediment fluxes results from the interaction of the main M_2 tide and internally generated overtides. Prescribing an M_4 overtide, a different type of balance, due to interactions between the main M_2 tide and the externally prescribed overtides, can be found. Since the morphological development in the different models is qualitatively the same and controlled by the same physical processes, it can be inferred that the same processes determine the equilibrium and evolution in the process-based model.

The model adaptations in water motion and sediment transport have no qualitative influence on the morphodynamic results. Hence, the simplifications in these formulations as used in the idealized model are justified. Only the adaptations of the boundary condition of the bed at the entrance have qualitative influence on the morphodynamic equilibria: the existence of equilibria in the process-based model strongly depends on this boundary condition. However, none of the model formulations is considered to adequately describe the natural behaviour at this point. Therefore, it is recommended to extend the model region to include (at least) the ebb-tidal delta when studying the evolution of tidal basins.

Appendix. Model formulations

In this Appendix, the main model formulations of the process-based model Delft3D-MOR, the adaptations in the intermediate model and the remaining differences with the idealized model are described.

In this study, the water motion is simulated in a one-dimensional model and the influence of Coriolis, density differences and wind or waves are neglected. The equation for conservation of momentum in the Delft3D model can therefore be simplified to:

$$\frac{\partial u}{\partial t} + u \frac{\partial u}{\partial x} + g \frac{\partial \eta}{\partial x} + \frac{gu|U|}{C^2(d+\eta)} - \nu \frac{\partial^2 u}{\partial x^2} = 0, \quad (1)$$

and the continuity equation is given by:

$$\frac{\partial \eta}{\partial t} + \frac{\partial u(d+\eta)}{\partial x} = 0, \quad (2)$$

in which:

- C : Chézy coefficient ($\text{m}^{1/2} \text{s}^{-1}$)
- d : water depth w.r.t. MSL (m)
- g : gravitational acceleration ($\text{m}^2 \text{s}^{-1}$)
- u : depth-averaged velocity (m s^{-1})
- U : magnitude of total velocity (m s^{-1})

- ρ : mass density of water (kg m^{-3})
- ν : diffusion coefficient (eddy viscosity) ($\text{m}^2 \text{s}^{-1}$)
- η : water level (m).

In the idealized model these shallow-water equations are also applied, but the last term in Eq. (1) is neglected because it is very small ($\nu = 1$). The friction term is linearized according to the energy, dissipation condition of Zimmerman (1992). In the intermediate model the friction term in Eq. (1) is replaced by this linearized term:

$$\hat{r} \frac{u}{d+\eta} \quad \text{with} \quad \hat{r} = \frac{8U_r C_D}{3\pi} \quad \text{and} \quad U_r = \frac{A\sigma L}{H}, \quad (3)$$

in which:

- \hat{r} : linearized friction coefficient (m s^{-1})
- U_r : characteristic velocity scale (m s^{-1})
- C_D : drag coefficient, g C^2
- A : tidal amplitude (m)
- σ : tidal frequency (s^{-1})
- L : length of estuary (m)
- H : depth of estuary at the mouth (m).

For small depths this friction term is expanded in the idealized model as:

$$\frac{\hat{r}u}{1-\alpha h} (1-\epsilon\eta), \quad (4)$$

in which $\epsilon = A/H$ is a small parameter and α is a factor close to 1 which prevents the term from becoming infinite for small water depths. The expansion is valid if $1-\alpha h \gg \epsilon\eta$. In the intermediate model this expansion is not applied. Instead, a drying and flooding procedure is used when a minimal water depth is reached. The shallow part is represented by removing grid cells that become dry when the tide falls, and reactivating cells that become wet when the tide rises. This difference in model description can lead to deviations in the water motion.

Additionally, deviations in the water motion can occur due to those non-linear interactions which result in M_6 and higher overtides. These are taken into account in the intermediate model and neglected in the idealized model.

The sediment transport in Delft3D-MOR consists of a suspended part and a bed-load part. Similarly to the idealized model, the bed-load transport is set to zero in the intermediate model. The depth-averaged advection-diffusion equation is used to calculate the suspended load transport. For the one-dimensional model this equation is given by:

$$\frac{\partial hc_s}{\partial t} + u \frac{\partial hc_s}{\partial x} + \frac{\partial}{\partial x} \left(\epsilon_x h \frac{\partial c_s}{\partial x} \right) = w_s \Gamma (c_e - c_s), \quad (5)$$

in which:

- ϵ_x : dispersion coefficient ($\text{m}^2 \text{s}^{-1}$)
- c_s : concentration of suspended sediment in volume sediment per volume water ($\text{m}^3 \text{m}^{-3}$)
- c_e : equilibrium concentration of suspended sediment ($\text{m}^3 \text{m}^{-3}$)
- w_s : fall velocity of suspended sediment (m s^{-1})

Γ : coefficient depending on w_s , u and bed shear stress velocity (-).

In the idealized model, a parametrization of the resuspended processes is used in the right-hand term of the depth-integrated advection-diffusion equation, given by:

$$\frac{\partial C_s}{\partial t} + u \frac{\partial C_s}{\partial x} + \frac{\partial}{\partial x} \left(\epsilon_x \frac{\partial C_s}{\partial x} \right) = \alpha_e u^2 - \gamma C_s, \quad (6)$$

in which α_e is the pick-up function, related to sediment properties, and γ is the deposition coefficient, related to settling velocity and vertical mixing. Whereas in the intermediate model the depth-averaged concentration c_s is used as variable, this model uses the depth-integrated concentration $C_s = c_s h \rho_s$ as variable. Here, ρ_s is the density of the sediment. This parameter is included, because in the idealized model the mass of the sediment is used in the formulations and in Delft3D-MOR its volume.

Delft3D-MOR uses a suspended sediment transport formula to calculate the equilibrium concentration c_e in Eq. (5). The parameterization of the idealized model is adopted in the intermediate model to calculate c_e . For an equilibrium state of the basin, the deposition equals the erosion, thus $C_s = \alpha_e / (\gamma u^2)$. To allow for the differences in dimensions between the two models, c_e in the intermediate model is calculated by:

$$c_e = \frac{\alpha_e}{\gamma \rho_s H} U^2, \quad (7)$$

in which the depth at the entrance, H , is used to represent the depth. Note that H is constant, while in the idealized model the local depth is used. This gives a difference in model formulations. When the basin is not in equilibrium, the formulations also differ in the factor in front of the parameterized term. This factor contains the parameter Γ which is depth-dependent in the intermediate model, while the factor γ is depth-independent in the idealized model. This results in a time scale which still depends on the local depth in the intermediate model, while it is constant in the idealized model.

At the seaward boundary, the intermediate model applies a dynamic evolving concentration:

$$\frac{\partial h c_s}{\partial t} = w_s \Gamma (c_e - c_s). \quad (8)$$

The description of the suspended-sediment concentration differs slightly from the idealized model. In this model a distinction between the time-averaged and time-varying part of the concentration is made. For the time-averaged part, the erosion is equal to the deposition. For the time-varying part, Eq. (6) is solved without diffusion, thus $\epsilon_x = 0$.

The bed-level variations result from gradients in the sediment transport, based on the conservation of sediment mass. In both models the bed evolution is given by:

$$(1 - \epsilon_{\text{por}}) \frac{\partial z_a}{\partial t} + \frac{\partial S_x}{\partial x} = 0, \quad (9)$$

in which:

z_a : bed level (m)

S_x : sediment transport in x direction ($\text{m}^3 \text{m}^{-2} \text{s}^{-1}$)

ϵ_{por} : bed porosity.

The bed level at the open boundary point is fixed independently of the sediment transport direction in the idealized model, while in Delft3D-MOR the bottom level is only fixed if the residual sediment transport is directed into the basin. In the intermediate model the condition of the idealized model is adopted.

Summarized, the friction term, the sediment-transport formulation and the fixation of the bed at the open boundary are adapted in the intermediate model. The remaining differences in the flow computations concern the generation of higher-order non-linear terms and the drying and flooding procedures at intertidal areas. In the sediment transport the models differ on (1) the parameterization of the erosion and deposition term, (2) the depth-integrated versus depth-averaged concentration in the advection-diffusion equation and (3) the boundary layer at the open boundary.

Acknowledgements The work presented here was done in the framework of the DIOC programme Hydraulic Engineering and Geohydrology of Delft University of Technology, Project 1.4. It is embedded as such in Project 03.01.03 (Coasts) of the Delft Cluster strategic research programme on the sustainable development of low-lying deltaic areas. This research was supported by NWO-ALW grant no. 810.63.12.

References

- De Vriend HJ (1996) Mathematical modelling of meso-tidal barrier island coasts. part I: Empirical and semi-empirical models. In: Liu PL-F (ed) Advances in coastal and ocean engineering. World Scientific, Singapore
- Lanzoni S, Seminara G (2002) Long-term evolution and morphodynamic equilibrium of tidal channels. *J Geophys Res* 107: 1–13
- Officer CB (1976) Physical oceanography of estuaries (and associated coastal waters). Wiley, New York
- Pritchard D, Hogg AJ, Roberts W (2002) Morphological modelling of intertidal mudflats: the role of cross-shore tidal currents. *Continental Shelf Res* 22: 1887–1895
- Roelvink JA, van Banning CKFM (1994) Design and development of Delft3D and application to coastal morphodynamics. In: Verwey A, Minns AW, Babovic V, Maksimovic C (eds) Hydroinformatics '94. Balkema, Rotterdam
- Schuttelaars HM, De Swart HE (1996) An idealized long-term morphodynamic model of a tidal embayment. *Eur J Mech (B) Fluids* 15(1): 55–80
- Schuttelaars HM, De Swart HE (2000) Multiple morphodynamic equilibria in tidal embayments. *J Geophys Res* 105: 24105–24118
- Thoolen PMC, Wang ZB (1999) Sediment transport modelling for the Western Scheldt. Tech Rep Z2649, WL|Delft Hydraulics, Delft
- Van Leeuwen SM, Schuttelaars HM, De Swart HE (2000) Tidal and morphologic properties of embayments: Effects of sediment deposition processes and length variation. *Phys Chem Earth (B)* 25: 365–368
- Wang ZB (1992) Some considerations on the mathematical modelling of morphological processes in tidal regions. In: Prandle D

- (ed) Dynamics and exchanges in estuaries and the coastal zone. Physics of Estuaries and Coastal Seas, 1990
- Wang ZB, Louters T, De Vriend HJ (1992) A morphodynamic model for a tidal inlet. In: Arcilla AS, Pastor M, Zienkiewicz OC (eds) Computing modelling in ocean engineering '91. Proceedings of the 2nd International Conference, 1991. Balkema, Rotterdam
- Wang ZB, Louters T, De Vriend HJ (1995) Morphodynamic modelling for a tidal inlet in the Wadden Sea. Mar Geol 126: 289–300
- Zimmerman JTF (1992) On the Lorentz linearization of a nonlinearly damped tidal Helmholtz oscillator. Proceeding Kon Ned Akad v Wetensch 95: 127–145